

[Article ID] 1003– 6326(2002) 04– 0780– 05

# High temperature deformation of L1<sub>2</sub>-FCC two phase Ir-15Nb-Ni refractory superalloys<sup>①</sup>

Y. F. Gu, Y. Yamabe-Mitarai, S. Nakazawa, H. Harada

(National Institute for Materials Science, 1-2-1 Sengen, Tsukuba, Ibaraki 305-0041, Japan)

**[Abstract]** The creep behaviors of the Ni-added Ir<sub>85</sub>Nb<sub>15</sub> alloys were investigated at 1 650~ 1 800 °C by compression tests in vacuum. X-ray diffractometry, transmission electron microscopy and scanning electron microscopy were conducted to characterize the microstructure and lattice misfit change by the addition of Ni in the Ir<sub>85</sub>Nb<sub>15</sub> alloy. The results reveal that the Ni addition has a significant effect on the creep resistance of the Ir<sub>85</sub>Nb<sub>15</sub> two phase refractory superalloys. Basing on the results, the relationship among the Ni addition, lattice misfit, microstructure development, and the creep behavior in the Ni-added Ir<sub>85</sub>Nb<sub>15</sub> alloys is discussed.

**[Key words]** refractory superalloy; microstructure; lattice misfit; creep behavior

**[CLC number]** TG 146.3; TG 132.3

**[Document code]** A

## 1 INTRODUCTION

Some Ir-based two-phase alloys, which have coherent FCC/L1<sub>2</sub>( $\gamma/\gamma'$ ) two-phase structure and are called refractory superalloys, are superior in high-temperature strength compared with Ir-based single-phase alloys, and have a good potential for use as structural materials in applications at ultra-high temperatures up to 1 800 °C<sup>[1~6]</sup>. However, binary Ir-based two-phase refractory superalloys normally fracture in an intergranular mode and subject to low crack tolerance at room temperature. High density and cost are also the primary barriers to their practical applications. The authors previously found that adding Ni effectively changes the fracture mode and improves the strength and compression ductility of an Ir<sub>85</sub>Nb<sub>15</sub> alloys, and that the density decreases by about 7% for every 10% Ir (mole fraction) replaced with Ni<sup>[6]</sup>.

Because the Ir-based two-phase refractory superalloys are intended for use as structural materials in ultra-high temperature applications, development of such alloys must consider high-temperature properties, such as creep resistance, and microstructural stability at ultra-high temperature. In this study, the effect of adding Ni on the creep behaviors of the Ir<sub>85</sub>Nb<sub>15</sub> alloy was determined at temperatures from 1650 °C to 1800 °C under 137 MPa, focusing on the relationship between the microstructural features and the creep resistances.

## 2 EXPERIMENTAL

Alloys of Ir<sub>85-x</sub>Nb<sub>15</sub>Ni<sub>x</sub> where  $x = 1, 5, 10$  were prepared using raw materials of 99.99% purity Ir, 99.98% purity Nb, and 99.5% purity Ni (mass fraction). The raw materials were mixed and pre-

pared as 50g button ingots by arc melting under argon in a vacuum furnace. Homogeneity of the ingots was ensured by re-melting the ingots at least 10 times.

Specimens with 6 mm in height and 3 mm in diameter were prepared by electron-discharge machine (EDM) from the ingots. These specimens were annealed at 1 800 °C for 72 h with furnace cooling under vacuum of about  $3 \times 10^{-4}$  Pa.

Constant-load compression creep tests were done on the polished samples at temperatures from 1 650 °C to 1 800 °C under a stress of 138 MPa in a vacuum by using an Instron 8560 testing machine. Graphite disks with 10 mm in diameter and 8 mm in height were used as spacers at both ends of the samples to prevent spontaneous welding between the samples and tungsten loading rods. The samples were heated to the test temperature over 2 h and then kept at that temperature for 15 min before testing. Creep strain was determined by using both a CCD camera and by measuring the load-strain displacement.

For studying the microstructure, these heat-treated and creep deformed samples were cut into disk samples (by using the EDM), which were then prepared by using conventional metallographic methods and examined by using a scanning electron microscope (SEM) and a transmission electron microscope (TEM). Accurate lattice parameters for the phases in the tested alloys were identified by using a high-resolution X-ray diffraction technique described in detailed elsewhere<sup>[7]</sup>.

## 3 RESULTS

Fig. 1 shows the typical micrographs of the tested alloys examined by using the SEM after annealing at 1 800 °C for 72 h (the bright phase is the  $\gamma$  phase

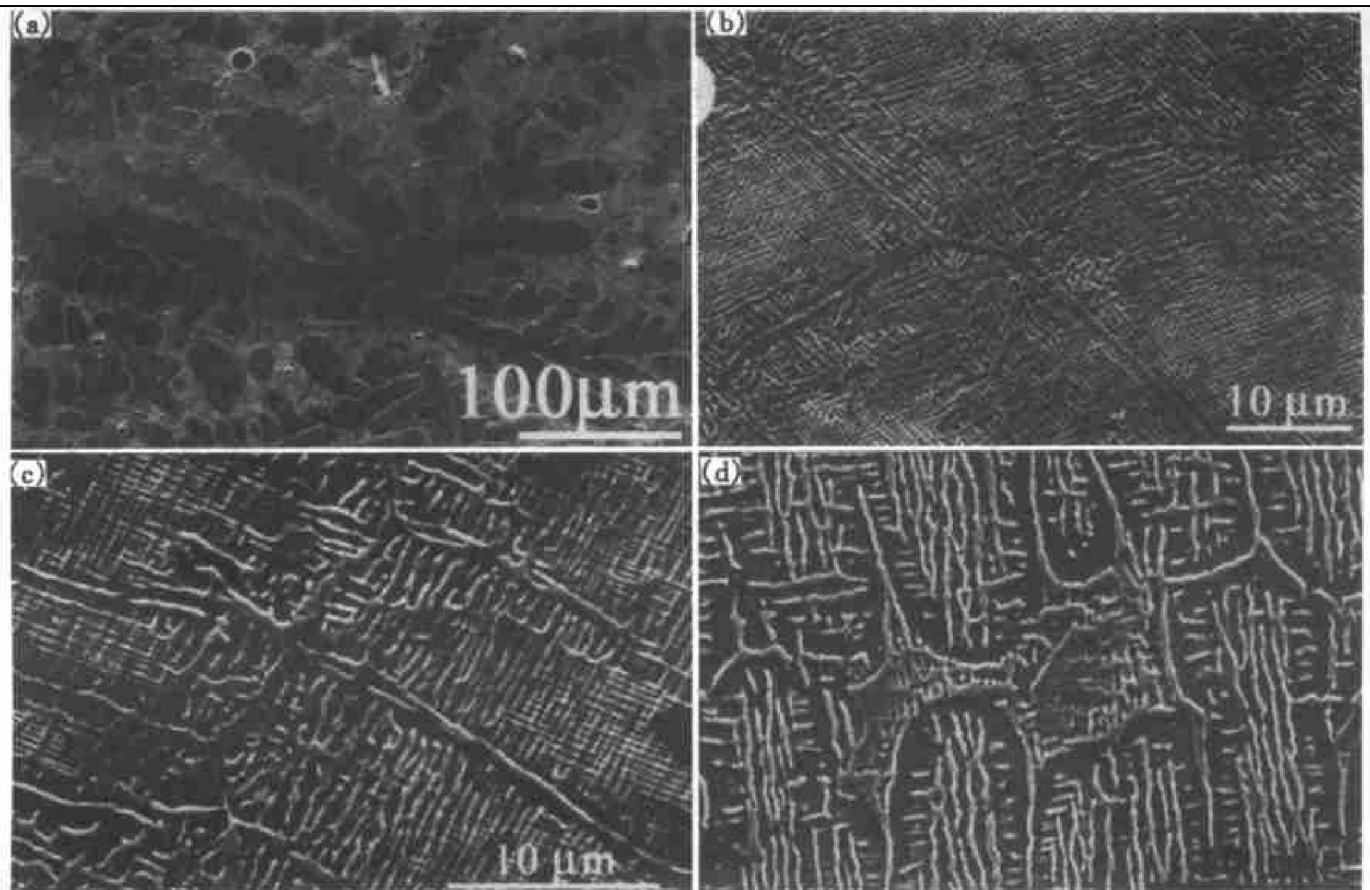


**Fig. 1** Micrographs of tested alloys after annealed at 1 800 °C for 72 h  
(a) —Ir<sub>85</sub>Nb<sub>15</sub>; (b) —Ir<sub>84</sub>Nb<sub>15</sub>Ni<sub>1</sub>; (c) —Ir<sub>80</sub>Nb<sub>15</sub>Ni<sub>5</sub>; (d) —Ir<sub>75</sub>Nb<sub>15</sub>Ni<sub>10</sub>

and the grey phase is the  $\gamma'$  phase). Grain size was similar for all tested alloys, about 250  $\mu\text{m}$ . The microstructures of all the tested alloys show a dendritic structure [as shown in Fig. 1(a)]. The  $\gamma + \gamma'$  two-phase structure, where the  $\gamma'$  phase sizes were varied from 0.3  $\mu\text{m}$  to 2  $\mu\text{m}$ , could be seen among dendritic and interdendritic areas [as shown in Figs. 1(b), 1(c) and 1(d)]. Larger sized  $\gamma$  and  $\gamma'$  phases, where the phase sizes varied from 1  $\mu\text{m}$  to 10  $\mu\text{m}$ , could be seen along some grain boundaries. These larger-sized phases increased with the Ni addition increasing.

The TEM investigation showed that the shape of the  $\gamma'$  phase for the tested alloys depended on the Ni content (as shown in Fig. 2). In the Ir<sub>84</sub>Nb<sub>15</sub>Ni<sub>1</sub> and Ir<sub>80</sub>Nb<sub>15</sub>Ni<sub>5</sub> alloys [as shown in Figs. 2(a) and 2(b)], the  $\gamma'$  precipitates were sphere with lattice misfit dislocation networks around the  $\gamma/\gamma'$  interface. However, in the Ir<sub>75</sub>Nb<sub>15</sub>Ni<sub>10</sub> alloy [as shown in Fig. 2(c)], the  $\gamma'$  precipitates were irregular, and some precipitates coalesced to form  $\gamma'$ -rods.

For the binary Ir<sub>85</sub>Nb<sub>15</sub> alloys, the XRD was used to determine Ni-induced changes in the phase constituents, lattice parameter and the volume fraction of the  $\gamma'$  phase. The peaks in the XRD patterns revealed that the alloys consisted only of the  $\gamma$  and  $\gamma'$  phases. Lattice parameters of the  $\gamma$  matrix and the  $\gamma'$  precipitate for the Ir<sub>85-x</sub>Nb<sub>15</sub>Ni<sub>x</sub> alloys were calculated by using the fundamental peaks from both the  $\gamma$  (FCC) and  $\gamma'$  (L1<sub>2</sub>) structures, and by using the

superlattice peaks only from the  $\gamma'$  (L1<sub>2</sub>) structure. The calculation indicated that the Ni addition of 1% (mole fraction) decreased the lattice misfit from about 0.44% (for the two-phase non-added Ir<sub>85</sub>Nb<sub>15</sub> alloy) to 0.25%. However, the lattice misfit increased subsequently with increasing Ni content, and was about 0.40% and 0.74% for the Ni addition of 5% and 10% (mole fraction), respectively. The calculation also indicated that the volume fraction of the  $\gamma'$  phase was relatively unaffected by the Ni addition (41% for the Ir<sub>85</sub>Nb<sub>15</sub> alloy and 39% for the Ir<sub>75</sub>Nb<sub>15</sub>Ni<sub>10</sub> alloy).

Creep tests were conducted in compression at temperatures from 1 650 °C to 1 800 °C under 137 MPa. Creep curves for the binary Ir<sub>83</sub>Nb<sub>17</sub> alloy and the Ir<sub>85-x</sub>Nb<sub>15</sub>Ni<sub>x</sub> alloys with  $x = 1, 5, 10$  at 1 650 °C are shown in Fig. 3. For the binary Ir<sub>83</sub>Nb<sub>17</sub> alloy and the Ni added Ir<sub>75</sub>Nb<sub>15</sub>Ni<sub>10</sub> alloy, experiments exhibited a visible primary creep and stable minimum strain rates over varying amounts of strains, followed by a tertiary stage with a rapid increase in the strain rate during testing period (298 h). However, for the Ir<sub>84</sub>Nb<sub>15</sub>Ni<sub>1</sub> and Ir<sub>80</sub>Nb<sub>15</sub>Ni<sub>5</sub> alloys, neither clear primary creep nor tertiary creep was observed and experiments exhibited stable strain rates over testing period (298 h for the Ir<sub>84</sub>Nb<sub>15</sub>Ni<sub>1</sub> alloy and 239 h for the Ir<sub>84</sub>Nb<sub>15</sub>Ni<sub>1</sub> alloy). The creep strain for the Ir<sub>84</sub>Nb<sub>15</sub>-Ni<sub>1</sub> alloy was about 1.2% when the creep testing stopped after 298 h. At 1 800 °C, the samples of the

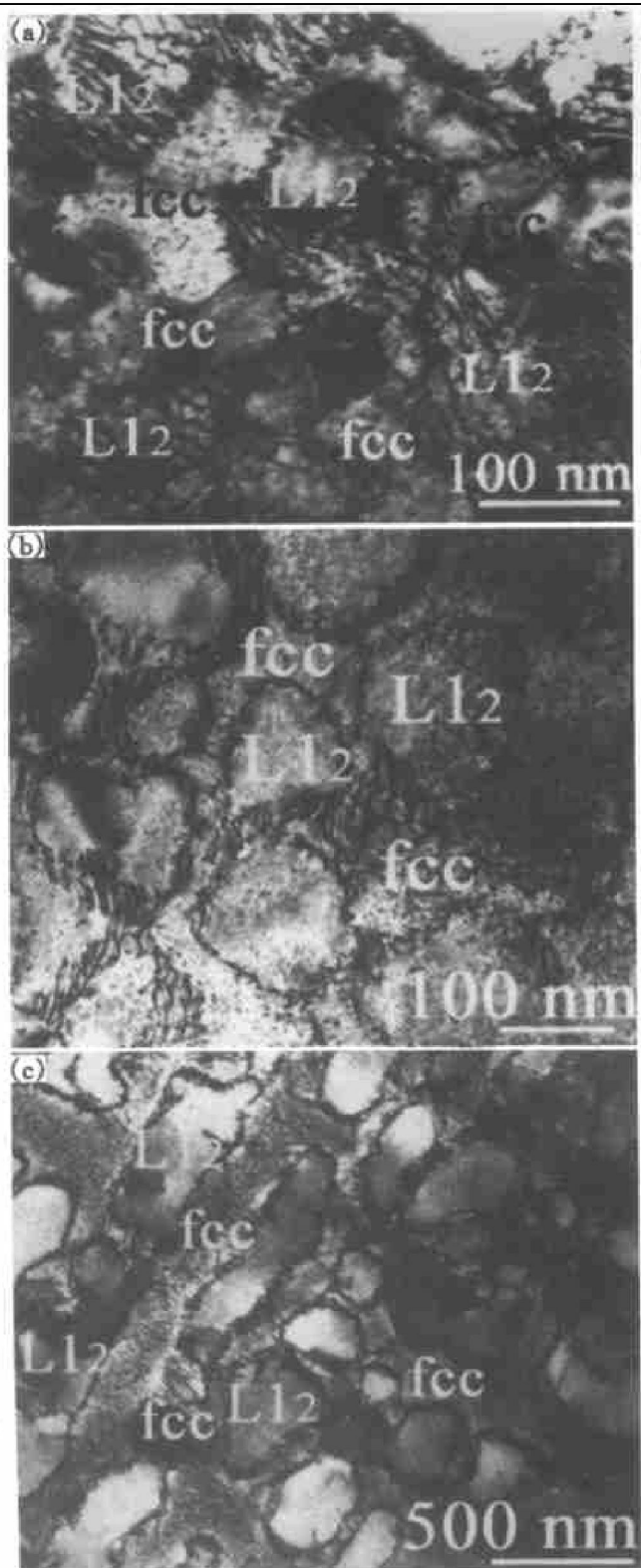


**Fig. 2** Typical micrographs of tested alloys illustrating L1<sub>2</sub> precipitate shape after annealed at 1 800 °C for 72 h

(a) —Ir<sub>84</sub>Nb<sub>15</sub>Ni<sub>1</sub>; (b) —Ir<sub>80</sub>Nb<sub>15</sub>Ni<sub>5</sub>; (c) —Ir<sub>75</sub>Nb<sub>15</sub>Ni<sub>10</sub>

binary Ir<sub>83</sub>Nb<sub>17</sub> alloy crushed down after 3 h testing with 5% strain<sup>[8]</sup>. The minimum creep rate during testing is  $2 \times 10^{-5} \text{ s}^{-1}$ . The Ni-doped Ir<sub>75</sub>Nb<sub>15</sub> alloys clearly exhibited primary creep and stable minimum strain rates over different creep time, followed by a tertiary stage with a rapid increase in the strain rate (as shown in Fig. 4). The Ir<sub>84</sub>Nb<sub>15</sub>Ni<sub>1</sub> alloy exhibited stable strain rate after 140 h testing, and the steady-

state creep strain rate was  $7.7 \times 10^{-8} \text{ s}^{-1}$ , about three orders of magnitude lower than that for the binary Ir<sub>83</sub>Nb<sub>17</sub> alloy<sup>[8]</sup>. The Ir<sub>75</sub>Nb<sub>15</sub>Ni<sub>10</sub> alloy crushed after about 6 h testing with 15% strain. Fig. 5 shows the steady-state creep strain rates for the Ni-added Ir<sub>85</sub>Nb<sub>15</sub> alloys at 1 650 °C, 1 730 °C and 1 800 °C under 137 MPa. All Ni-added Ir<sub>85</sub>Nb<sub>15</sub> alloys had lower steady-state creep strain rates than the non-added Ir<sub>85</sub>Nb<sub>15</sub> alloys at testing temperatures.

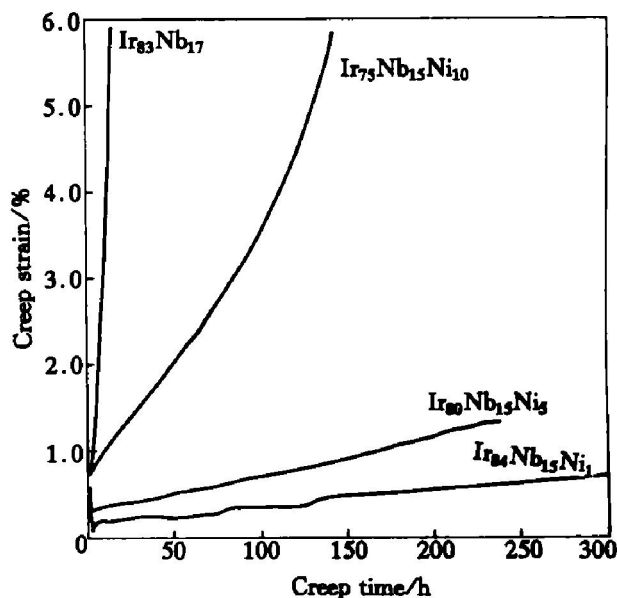


**Fig. 3** Creep curves for binary Ir<sub>83</sub>Nb<sub>17</sub> and Ir<sub>85-x</sub>Nb<sub>15</sub>Ni<sub>x</sub> with  $X = 1, 5, 10$  at 1 650 °C under 137 MPa

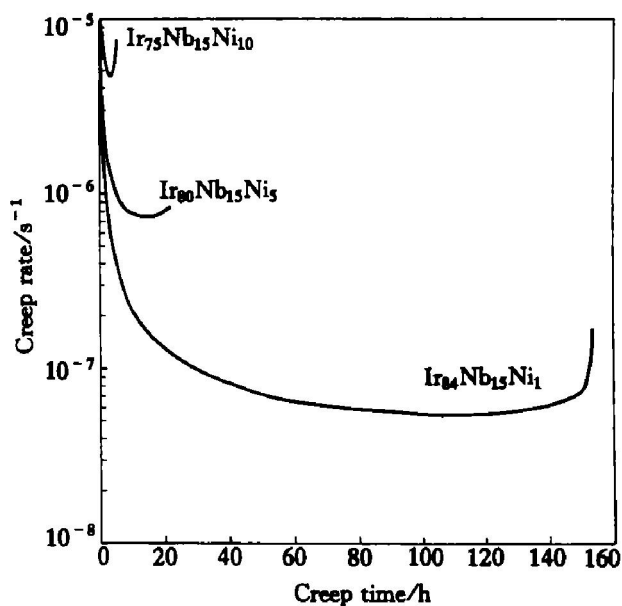


**Fig. 4** Creep rates for tested alloys at 1 800 °C under 137 MPa

Observation of the fractured surfaces after creep tests showed that in the binary Ir<sub>83</sub>Nb<sub>17</sub> alloy, cracks mainly initiated and propagated along the grain boundaries, whereas in the Ni-added Ir<sub>85</sub>Nb<sub>15</sub> alloys, cracks mainly propagated in a transgranular manner, namely, across grain boundaries.

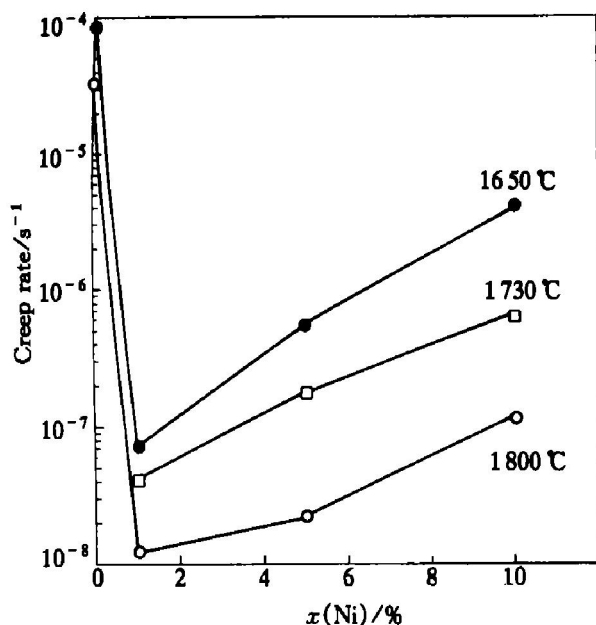


**Fig. 5** Creep rates for binary Ir<sub>83</sub>Nb<sub>17</sub> and Ir<sub>85-x</sub>Nb<sub>15</sub>Ni<sub>x</sub> with  $x = 1, 5, 10$  at various temperatures

#### 4 DISCUSSION

The results show that addition of Ni significantly affected the creep resistance of Ir<sub>85</sub>Nb<sub>15</sub> alloys. The addition of 1% Ni decreased the creep rate by about three orders of magnitude compared with the rate for non-added Ir<sub>83</sub>Nb<sub>17</sub> alloys. Although the detailed creep mechanism for Ni-added Ir<sub>85</sub>Nb<sub>15</sub> alloys remains unclear, the results reveal effects of Ni addition on the creep behavior of the alloys.

In general, the loss of creep resistance of polycrystalline  $\gamma + \gamma'$  two-phase alloys due to high-temperature creep is caused by the coarsening of  $\gamma'$  or by mechanical damage such as initiation and propagation of cracks at the grain boundary<sup>[9, 10]</sup>. Conley et al<sup>[11]</sup> found that elastic effects can influence  $\gamma'$  coarsening rates in Ni-base alloys and high magnitudes of misfit were correlated with increased coarsening rate. For the Ni-added Ir<sub>85</sub>Nb<sub>15</sub> alloys, the creep resistance might mainly depend on the evolution of the microstructure or the  $\gamma'$  coarsening process. The results in the current study show that the apparent lattice misfit for the binary Ir<sub>85</sub>Nb<sub>15</sub> decreased from 0.44% to 0.25% by the addition of 1% Ni and subsequent increased as Ni content was continuously raised up to 10%. The reasons for the lattice misfit development may come from the interface relaxation caused by adding Ni and the lattice parameter change caused by the distribution of the Ni in the phases. Because the  $\gamma'$  phase has larger lattice parameter in the tested alloys, an elastic constraint on the  $\gamma'$  phase from the  $\gamma$  matrix may easily relax for the alloy with 1% Ni [as shown in Fig. 2(a)]. As Ni content is increased, relaxation becomes more difficult owing to a solid solu-

tion in the  $\gamma$  matrix [as shown in Figs. 2(b) and 2(c)]. Meanwhile, because the size of Ni atom is about 10% smaller than that of either Ir or Nb, adding Ni decreases the lattice parameters of both the  $\gamma$  and  $\gamma'$  phases<sup>[6]</sup>. Decrease in the lattice parameter for both phases is decided by the dissolution content of Ni in the phases. If the dissolution content of added Ni is more in the  $\gamma'$  phase than that in the  $\gamma$  phase, the lattice parameter of the  $\gamma'$  phase will decrease greatly and thus the misfit decreases. It is therefore suggested that most of the added Ni enters into the  $\gamma'$  phase as Ni content is about 1%. With increasing Ni content, more and more added Ni dissolves into the  $\gamma$  phase due to the solid solution limit of Ni in the  $\gamma'$  phase and then caused the misfit between the  $\gamma$  and  $\gamma'$  phase increase again. The decrease in lattice misfit changed the  $\gamma'$  shape from a cube (for the binary Ir<sub>85</sub>Nb<sub>15</sub>) to a sphere (for the Ir<sub>84</sub>Nb<sub>15</sub>Ni<sub>1</sub> alloy) and induced a network of misfit dislocations formed at the  $\gamma/\gamma'$  interfaces (as shown in Fig. 5). This network might be beneficial to  $\gamma'$  stability and effective for preventing dislocation motion during creep tests. However, with increasing Ni addition, the lattice misfit for Ni-added alloys increased, and the  $\gamma'$  particles in the alloy with the larger lattice misfit easily became coarse during creep tests and then lost their resistance to dislocation motion, such as that exhibited by the Ir<sub>75</sub>Nb<sub>15</sub>Ni<sub>10</sub> alloy. In addition, because the compositions of the  $\gamma$  and  $\gamma'$  are different, the coarsening of the  $\gamma'$  particles must be accompanied by diffusion of alloy constituents (Ir, Nb, and Ni) between the faces normal and parallel to the applied compression. The coarsening rate is presumably controlled by the diffusion rate. Although the diffusion rate for Ni, Nb, and Ir atoms in the Ir-Nb-Ni alloy system at such high temperatures was not determined, the diffusion rate of the Ni atom is reasonable the highest among the three. Further addition of Ni would increase the rate of coarsening and thus make the alloys prone to degradation of creep resistance. Based on the results, the optimum addition of Ni to an Ir<sub>85</sub>Nb<sub>15</sub> alloy is less than 5% to obtain a Ni-added Ir<sub>85</sub>Nb<sub>15</sub> alloy that retains high strength at both room and high temperatures.

In addition, the previous results showed that the grain boundary in binary Ir-based alloys is a weak point and that cracks often initiate and propagate along the grain boundary<sup>[11]</sup>. It is also showed that the addition of Ni to an Ir<sub>85</sub>Nb<sub>15</sub> alloy can effectively change the fracture mode of the alloys. This change might be caused by the Ni addition strengthening the grain boundary and changing the structure around the grain boundary<sup>[6]</sup>. Because the mechanical damage during creep tests mainly occurred at the grain boundaries for the binary Ir<sub>83</sub>Nb<sub>17</sub> alloy but occurred inside the grain for the Ni-added Ir<sub>85</sub>Nb<sub>15</sub> alloys, the great-

est improvement in creep resistance resulting from Ni addition may be connected to this change in the crack behavior.

## 5 CONCLUSIONS

1) Steady-state creep rate for the  $\text{Ir}_{84}\text{Nb}_{15}\text{Ni}_1$  alloy was about three orders of magnitude lower than that for the binary  $\text{Ir}_{83}\text{Nb}_{17}$  alloy at testing temperatures.

2) Lattice misfit between the FCC matrix and the  $\text{L}_{12}$  precipitate changed from 0.41% for the binary  $\text{Ir}_{85}\text{Nb}_{15}$  alloy to 0.24% for the  $\text{Ir}_{84}\text{Nb}_{15}\text{Ni}_1$  alloy, 0.40% for  $\text{Ir}_{80}\text{Nb}_{15}\text{Ni}_5$ , and 0.78% for  $\text{Ir}_{75}\text{Nb}_{15}\text{Ni}_{10}$ .

3) Creep resistance significantly improved due to addition of 1% Ni addition, probably due to the decrease in the lattice misfit and the change in the crack behavior for Ni-added  $\text{Ir}_{85}\text{Nb}_{15}$  alloys, compared with that for the binary  $\text{Ir}_{83}\text{Nb}_{17}$  alloy.

## [ REFERENCES ]

- [ 1 ] Yamabe Y, Koizumi Y, Murakami H, et al. Development of Ir-base refractory superalloys [ J ]. Scripta Mat, 1996, 35(2): 211– 215
- [ 2 ] Yamabe-Mitarai Y, Koizumi Y, Murakami H, et al. Reactions of solid copper with pure liquid tin and liquid tin saturated with copper [ J ]. Scripta Mat, 1997, 36(4): 393– 398.
- [ 3 ] Yamabe-Mitarai Y, Koizumi Y, Murakami H, et al. Platinum group metals base refractory superalloys [ J ]. Mat Res Soc Symp Proc, 1997, 460: 701– 706.
- [ 4 ] Yamabe-Mitarai Y, Ro Y, Yokokawa T, et al. Platinum group metals base refractory superalloys for ultra-high temperature use [ J ]. Structural Intermetallics, 1997, 805– 814.
- [ 5 ] Yamabe-Mitarai Y, Ro Y, Maruko T, et al. Ir-base refractory superalloys for ultra-high temperature [ J ]. Met Trans, 1998, 29A: 537– 549.
- [ 6 ] Gu Y F, Yamabe-Mitarai Y, Ro Y, et al. Properties of the  $\text{Ir}_{85}\text{Nb}_{15}$  two-phase refractory superalloys with nickel additions [ J ]. Met Trans, 1999, 30: 2629– 2639.
- [ 7 ] Yoshitake S, Yokokawa T, Ohno K, et al. Materials for Advanced Power Engineering, Part ( I ) [ M ]. Kluwer Academic Publishers, Dordrecht, The Netherlands, 1994. 875– 882.
- [ 8 ] Yamabe-Mitarai Y, Nakazawa S, Harada H. CREEP 7, Proceeding of the 7th International Conference on Creep and Fatigue at Elevated Temperatures [ C ]. Tsukuba: JSME, 2001. 533.
- [ 9 ] Woodford D A. Creep damage and the remaining life concept [ J ]. J Eng Mater Technol, 1979, 101: 311– 316.
- [ 10 ] Shirya N, Keown S R. Correlation between rupture ductility and cavitation in Cr-Mo-V steels [ J ]. Met Sci, 1979, 13: 89– 93.
- [ 11 ] Conley J G, Fine M E, Weertman J R. Effect of lattice disregistry variation on the late stage phase transformation behavior of precipitates in Ni-Mo alloys [ J ]. Acta Metall, 1989, 37: 1251– 1263.

( Edited by YANG Bing )